Rheology of the Upper Mantle: A Synthesis

Article *in* Science · June 1993

DOI: 10.1126/science.260.5109.771 · Source: PubMed

2 authors:

Shun-ichiro Karato
Yale University
393 PUBLICATIONS **24,266** CITATIONS
SEE PROFILE

Patrick Wu
The University of Calgary
183 PUBLICATIONS **6,514** CITATIONS
SEE PROFILE

Rheology of the Upper Mantle: A Synthesis

Shun-ichiro Karato; Patrick Wu

Science, New Series, Vol. 260, No. 5109 (May 7, 1993), 771-778.

Stable URL:
http://links.jstor.org/sici?sici=0036-8075%2819930507%293%3A260%3A5109%3C771%3AROTUMA%3E2.0.CO%3B2-B

Science is currently published by American Association for the Advancement of Science.

ARTICLE

Rheology of the Upper Mantle: A Synthesis

Shun-ichiro Karato and Patrick Wu

Rheological properties of the upper mantle of the Earth play an important role in the dynamics of the lithosphere and asthenosphere. However, such fundamental issues as the dominant mechanisms of flow have not been well resolved. A synthesis of laboratory studies and geophysical and geological observations shows that transitions between diffusion and dislocation creep likely occur in the Earth's upper mantle. The hot and shallow upper mantle flows by dislocation creep, whereas cold and shallow or deep upper mantle may flow by diffusion creep. When the stress increases, grain size is reduced and the upper mantle near the transition between these two regimes is weakened. Consequently, deformation is localized and the upper mantle is decoupled mechanically near these depths.

The Earth is made of polycrystalline materials which, like ceramic materials, show a rich variety of rheological behavior depending on the conditions of deformation (*1*). At a relatively low stress level, small grain size, or both, deformation occurs through diffusive mass transport between grain boundaries (diffusion creep), and the strain rate increases linearly with stress (linear rheology) but decreases significantly with grain size. In contrast, at a high stress level, large grain size, or both, deformation occurs through the motion of crystalline dislocations within grains (dislocation creep), and the strain rate increases nonlinearly with stress (nonlinear rheology) but is insensitive to grain size. Deformation that is caused by dislocation creep results in preferred orientation of minerals and, therefore, anisotropy of seismic wave velocities (*2–4*) and creep strength (*5*); these changes do not occur in diffusion creep (*6*). Strain rates that are determined by both mechanisms are sensitive to temperature and pressure, but the magnitude of temperature and pressure effects is generally different between the two. For a given temperature and pressure, the mechanism that gives the higher strain rate becomes the dominant creep mechanism. Therefore, the dominant mechanisms of deformation may also change with depth or with regional temperatures (geothermal gradients).

Theoretical studies showed that the dynamical behavior of the Earth's interior depends critically on rheological flow laws. For example, the pattern of mantle convection is sensitive to the stress dependence of creep rate: Flow is more localized with nonlinear than with linear rheology (*7*), and more distinct spatial and temporal variation of flow is observed in materials with nonlinear rheology than in those with linear rheology (*8*). In addition, the difference in grain size dependence may also cause a difference in shear localization: When a material is subject to or close to the conditions in which flow that is sensitive to grain size occurs, then a decrease in grain size will cause a significant enhancement of creep rate that will lead to a localization of deformation (*9*). Further, the depth variation of viscosity is sensitive to the stress dependence of strain rate, when the strain rate or energy dissipation rate is constant with depth (*10*).

Despite these effects of flow laws on mantle dynamics, the flow laws of the Earth's mantle have not been well constrained. This uncertainty results from the inherent difficulties in the studies of rheological properties. The most direct estimation of the rheological properties of the Earth comes from deformation experiments on rocks in laboratories at high temperatures and pressures. Most of the earlier studies on deformation of upper mantle rocks showed evidence for dislocation creep (*11*) and the flow laws for dislocation creep have often been extrapolated to lower strain rates and higher pressures of the Earth (*12*). However, this approach has two major difficulties, and the results are subject to large uncertainties. There are difficulties in conducting deformation experiments at high confining pressures (*13*). Most of the previous laboratory studies on rock deformation or related properties (such as diffusion) were made at relatively low pressures (<3 GPa), and the large extrapolations in pressure that are necessary for the application of these results to the Earth resulted in large uncertainties. The other, more essential, point is that almost all deformation experiments are made at much shorter time scales and so at much larger stresses than are present in the deformation processes in the Earth. These conditions mean that the laboratory results must be extrapolated to shorter time scales or to lower stresses when applied to the Earth, and possible changes in the deformation mechanisms at lower stress levels raise questions as to the validity of extrapolation. Some theoretical studies were made to estimate the relative importance of dislocation and diffusion creep (*15*) but were made on the basis of empirical correlations and not direct laboratory measurements. The transition conditions between dislocation and diffusion creep in olivine were directly determined with the use of synthetic specimens in which diffusive mass transport between grain boundaries is enhanced by the small grain size (*16*). The transition conditions between dislocation and diffusion creep are close to the conditions of the Earth's upper mantle. This relation means that a subtle change in deformation conditions changes the dominant deformation mechanism, but this study was made at low pressure (300 MPa), and the extrapolation to the higher pressures in the deep upper mantle was difficult.

Deformation microstructures of upper mantle rocks can be used to decipher the dominant deformation mechanisms. Most of the rocks from the upper mantle show evidence for dislocation creep: strong preferred orientation of minerals as well as dislocation structures similar to those in experimentally deformed rocks in the dislocation creep regime (*17*). However, the use of these microstructures has two major limitations: First, the maximum depth from which upper mantle rocks are carried is usually limited to ~200 km [(*18*); however, see (*19*)]. Thus, the deformation mechanisms in the deep upper mantle (>200 km) usually cannot be inferred from this type of study. Second, microstructures in these rocks reflect mostly the deformation processes associated with upward transfer of these rocks, which have significantly shorter time scales than the plate tectonic processes (*20*). Therefore, deformation mechanisms at longer time scales, and so at lower stresses, are difficult to infer through microstructural studies.

An alternative way to estimate the rheological properties of the Earth is through analysis of some time-dependent deforma-

S. Karato is in the Department of Geology and Geophysics, University of Minnesota, Minneapolis, MN 55455. P. Wu is in the Department of Geology and Geophysics, University of Calgary, Calgary, Alberta, Canada T2N 1N4.

tion processes of the Earth, such as postglacial rebound caused by the melting of ice sheets (*21*). The melted water entered the oceans and loaded the ocean basins. This change in surface load caused the vertical movement of the crust, which is recorded as the relative sea level (RSL) data. This record shows temporal variation due to the change in surface load and the mass of the seawater and to the viscous time-dependent flow of mantle materials. Thus, from the melting history of ice sheets, theoretical analysis of this relaxation process yields information about the rheological properties of the Earth's interior. Usually the Earth is modeled as a stratified viscoelastic material with linear rheology. This approach can provide a precise value of average effective viscosity (*22*) of the Earth [$\sim 1 \times 10^{21}$ Pa·s; see (*21*)]. However, some details remain controversial, such as the rheological constitutive relation, namely, the stress dependence of strain rate (*23*). Because nonlinear dislocation creep has been observed in most of the laboratory studies, some theoretical studies have been made to test the validity of nonlinear rheology in the analysis of postglacial rebound (*24*). However, these earlier models made some simplifying assumptions that have been shown as unjustifiable (*25*).

Thus, the deformation mechanisms and the resultant rheological constitutive relations in the Earth's mantle appear to have been poorly constrained. However, significant progress has been made in various areas of earth science to constrain the rheological properties of the Earth's upper mantle. First, the diffusion coefficients relevant to mass transfer in olivine have been determined for conditions that approach those of the deep upper mantle (*26*). These values make it possible to estimate the creep strength that results from diffusion creep down to these depth ranges without extrapolation of pressure and temperature. Second, seismic anisotropy, which reflects preferred orientation of minerals and so is sensitive to deformation mechanisms, has been investigated with the use of surface waves with long wavelengths, which "see" deeper into the mantle (*27, 28*). Third, new developments have been made in the numerical analysis of postglacial rebound (*25*), which make it possible to test the stress dependence of flow. The purpose of this article is to unite these new developments into a unified view of upper mantle rheology and to explore its possible implications for mantle dynamics.

Plastic Flow in Olivine

The major minerals in the upper mantle include olivine, orthopyroxene, clionopyroxene, and garnets (*29*). Of these, olivine is the most abundant and probably the weakest under a wide range of conditions as shown by both laboratory studies (*11, 30*) and microstructural analyses of naturally deformed peridotites (*31*). Thus, the rheology of the upper mantle is probably dominated by that of polycrystalline olivine. At steady state, the strain rate ($\dot{\epsilon}$) of rocks depends on temperature (T), pressure (P), grain size (d), and shear stress (σ) as

$$\dot{\epsilon} = A(\sigma/\mu)^n(b/d)^m\exp[-(E^* + PV^*)/RT] \quad (1)$$

where A is the preexponential factor, μ is the shear modulus (~80 GPa), b is the length of the Burgers vector (~0.5 nm), n is the stress exponent, m is the grain-size exponent, E^* is the activation energy, V^* is the activation volume, and R is the gas constant (Table 1).

Olivine polycrystals show either dislocation or diffusion creep, depending on the range of parameters. As shown in Table 1, each rheology is associated with specific parameters: dislocation creep has a larger stress exponent, smaller grain-size exponent, higher activation energy, and higher activation volume than those of diffusion creep (*32*). These differences mean that diffusion creep dominates over dislocation creep at relatively low stress, small grain size, low temperature, and high pressure. However, some of the parameters in the flow law are poorly constrained, such as the activation volume for dislocation creep (*33*). Therefore, we have used a range of values to show the effect of varying activation volume.

Among the various chemical conditions that affect creep in olivine, water fugacity (or water content) has a large effect and varies greatly with tectonic setting. Water content in the upper mantle has been inferred from that in basalts (*34*) and from infrared spectroscopy on mantle minerals (*35*). These studies, combined with the laboratory study of water solubility in olivine (*36*), indicate that the upper mantle beneath the mid-ocean ridges is undersaturated with water (<0.01% by weight), whereas the upper mantle beneath the island arcs is presumably saturated with water (~0.03% by weight). Olivine (and orthopyroxene and clionopyroxene) from subcontinental mantle also shows variable amounts of water but less than the solubility limit (*35*). Electrical conductivity of olivine is also likely to increase with water content (*37*). The small electrical conductivity ($\sim 10^{-3}$ S m^{-1}) of the suboceanic upper mantle that has been observed (*38*)

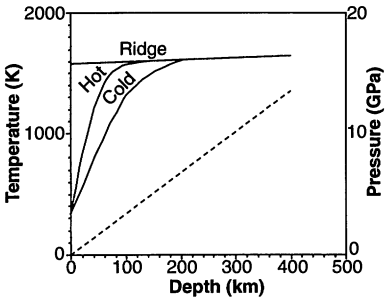

Fig. 1. Three representative geotherms (solid traces) and pressure distribution (dotted trace) in Earth's upper mantle for a ridge, a young (~30 million years) suboceanic upper mantle (hot), and an old (~150 million years) suboceanic upper mantle, or continental shield (cold).

Table 1. Flow law parameters for olivine. Dry means water-free and wet means water-saturated conditions. Flow law parameters are less well constrained at wet conditions than at dry conditions. Functional form of pressure dependence may also be different from that in Eq. 1 under wet conditions.

Mechanism	Dry	Wet
Dislocation creep		
A (s^{-1})	3.5×10^{22}	2.0×10^{18}
n	3.5	3.0
m	0	0
E^* (kJ mol^{-1})	540	430
V^* (cm^3 mol^{-1})	15 to 25†	10 to 20†
Diffusion creep		
A (s^{-1})	8.7×10^{15}	5.3×10^{15}
n	1.0	1.0
m	2.5‡	2.5‡
E^* (kJ mol^{-1})	300	240
V^* (cm^3 mol^{-1})	6§	5§

†The activation volume for dislocation creep is not well constrained. Values from 13 cm^3 mol^{-1} at wet conditions to 27 cm^3 mol^{-1} at nearly dry conditions have been reported (*33*). Considering this uncertainty, we used a range of activation volumes, 15 to 25 cm^3 mol^{-1} for dry olivine and 10 to 20 cm^3 mol^{-1} for wet olivine. ‡The grain-size exponent is reported as 2 for dry olivine and 3 for wet olivine (*16*). However, during extrapolation to a large grain size, the grain-size exponent may change from 2 to 3 or from 3 to 2 (*16*). Taking this uncertainty into account, we chose a grain-size exponent of 2.5, and the preexponential factors were modified accordingly. §The activation volume for diffusion is determined as 6 cm^3 mol^{-1} at dry conditions (*26*). No data are available for the activation volume for diffusion at wet conditions; we assumed that this value is ~80% of the activation volume at dry conditions.

indicates that this region is not saturated with water, supporting the conclusion made on the basis of water content in basalts.

Thus, we conclude that the rheology of the suboceanic and subcontinental upper mantle is between that of dry (water-free) and wet (water-saturated) olivine, whereas the rheology of the upper mantle under island arcs is close to that of wet olivine. The flow law of olivine in the presence of water is not well established, but the available laboratory observations indicate that the presence of water enhances both dislocation and diffusion creep by roughly the same magnitude (*16*). This similarity means that, for a given stress, the transition depth between dislocation and diffusion creep does not depend much on water content. However, at a given strain rate, the conditions under which diffusion creep dominates expand when a significant amount of water is present, because stress necessary to deform at a given strain rate is lower.

The viscosities corresponding to these two deformation mechanisms in the mantle vary according to the geothermal gradients (Fig. 1) (*39*). Also, viscosities for dislocation creep depend on the highly uncertain activation volume. However, some general features can be observed: Viscosities for dislocation creep decrease with depth to a sharp minimum and then increase, whereas viscosities for diffusion creep have only a weak dependence with depth $<\sim 100$ to 150 km (Fig. 2). The conditions in the mantle where deformation by each mechanism dominates can be calculated by comparison of the viscosities for the two deformation mechanisms (Fig. 3). The geothermal gradient has an important effect on the rheological transition. In the shallow upper mantle near mid-ocean ridge, the dominant deformation mechanism is dislocation creep. However, as the geothermal gradient decreases, diffusion creep becomes dominant in the shallow, relatively cold upper mantle.

In applying the results given in Fig. 3, A, C, and E, to the mantle, one needs to consider the processes controlling grain size in the Earth, namely, dynamic recrystallization and grain growth (*40*). Grain growth occurs in both the dislocation and diffusion creep regimes, whereas dynamic recrystallization occurs only in the dislocation creep regime (*41*). Grain size controlled by growth is independent of stress (*42*), but grain size controlled by dynamic recrystallization depends on stress magnitude. At steady-state deformation, grain size is given by

$$d = Kb(\sigma/\mu)^{-q} \qquad (2)$$

where K (19) and q (1.2) are nondimensional constants that are insensitive to temperature (*43*). Thus, when the deformation conditions are within the dislocation creep regime, grain size is defined as the value given by Eq. 2 that is determined by the stress magnitude. Both the recrystallized grain size, d_r (determined with Eq. 2), and the grain size at the transition from dislocation to diffusion creep, d_t (shown in Fig. 3, A, C, and E) decrease with stress, but at some point $d_t = d_r$ because d_r decreases faster with stress than does d_t (Fig. 4) (*44*). Thus, as the stress level increases, deformation in the dislocation regime makes grain size small enough to promote diffusion creep ($d_t > d_r$) (Fig. 4).

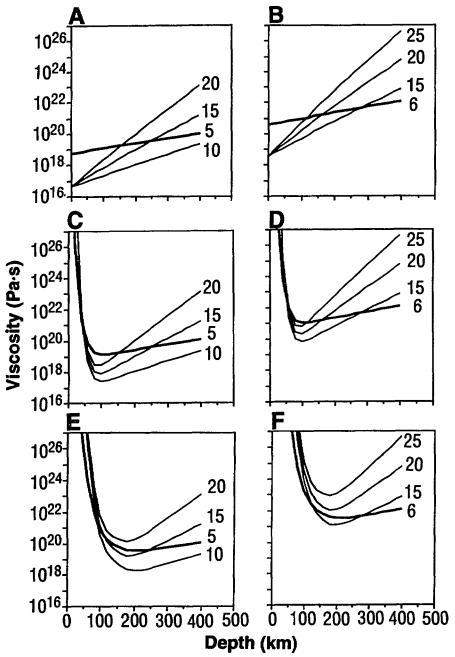

Fig. 2. Depth variation of effective viscosity for various geotherms and a range of activation volumes for dislocation creep. (**A**) Ridge, wet; (**B**) ridge, dry; (**C**) hot, wet; (**D**) hot, dry; (**E**) cold, wet; (**F**) cold, dry. Thick traces represent diffusion, and thin traces represent dislocation. The numbers by the traces are the activation volumes (in cubic centimeters per mole; Table 1). Effective viscosity for nonlinear dislocation creep depends on stress level, and effective viscosity for diffusion creep depends on grain size. A reference stress of 1 MPa and a reference grain size d_o of 1 mm are assumed in this calculation. At a different stress or grain size, viscosity can be calculated as $\eta_o(\sigma/\sigma_o)^{1-n}(d/d_o)^m$. Viscosity for dislocation creep has a minimum at a depth of 100 to 200 km (depending on the assumed geotherm and the activation volume) and increases significantly below that depth. In contrast, viscosity for diffusion creep changes little in the deep upper mantle.

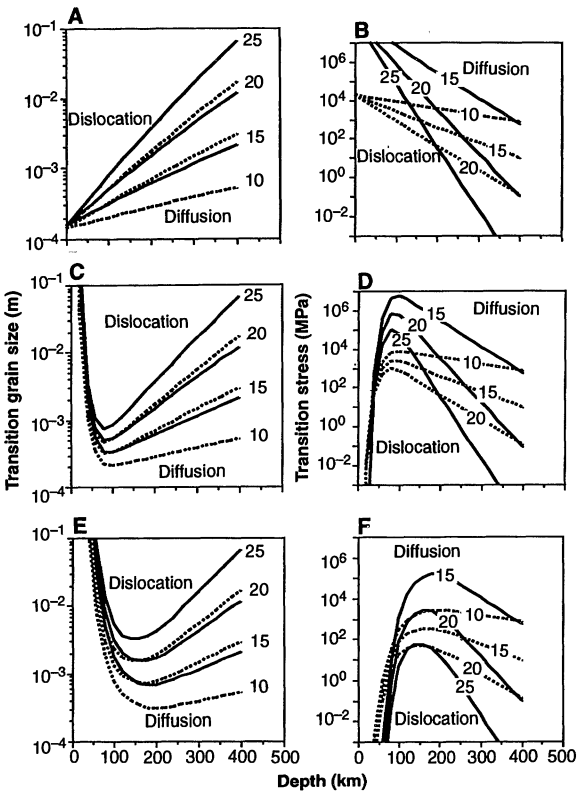

Fig. 3. Transition conditions of rheological behavior between linear (diffusion creep) and nonlinear (dislocation creep) rheology. The crossover points in Fig. 2 between viscosity for dislocation and for diffusion creep give the transition conditions between the two. Labels for these two mechanisms define the region where each operates. The activation volume (cubic centimeters per mole) for dislocation creep appears by each trace. Two cases are shown: (**A**, **C**, and **E**) Grain size and stress are independent parameters. For a given activation volume for dislocation creep, the dominant deformation mechanism is dislocation creep when the grain size is larger than the transition grain size shown in the diagram. Transition grain sizes (d_{to}) are shown at a reference stress of 1 MPa. At a different stress level, the transition grain size is $d_{to}(\sigma/\sigma_o)^{(1-n)/m}$. (**B**, **D**, and **F**) Grain size is determined by the stress through dynamic recrystallization. When the stress is larger than the transition stress, recrystallized grain size is small enough to promote diffusion creep; below that stress, the deformation mechanism remains dislocation creep. At ridges (A and B), the dominant deformation mechanism is almost always dislocation creep at shallow depths, whereas at deeper portions diffusion creep is dominant. The dominant deformation mechanism for other colder geotherms at relatively shallow but hot regions is dislocation creep, but the mechanism changes into diffusion creep in the cold and shallow upper mantle or deep upper mantle. (C and D) Hot upper mantle; (E and F) cold upper mantle. Solid traces, dry; dotted traces, wet.

The likely parameter values for the mantle suggest that deformation occurs by dislocation creep in the shallow upper mantle beneath ocean ridges or at intermediate depths in the hot or cold mantle, whereas deformation occurs by diffusion creep in the cold, shallow upper mantle or deep upper mantle (Fig. 3). However, the exact depths of transition depend on poorly known parameters such as the activation volume for dislocation creep, grain size, or stress.

Lattice Preferred Orientation and Seismic Anisotropy

Deformation mechanisms may also be inferred from the microstructures of rocks. Among the various microstructures, the most diagnostic for deformation mechanisms is the lattice preferred orientation (LPO). Minerals become oriented in a rock when it is deformed by dislocation creep (*2–4*) but assume an isotropic distribution when deformation occurs by diffusion creep (*6*). Preferred orientation of elastically anisotropic minerals (such as olivine and the pyroxenes) causes an anisotropy in the propagation of seismic waves (*2–4*). Thus, we can use both the LPO measurements on naturally deformed rocks and the observations of seismic anisotropy to infer the dominant deformation mechanisms and flow patterns in different parts of the mantle. In the major portions of the mantle where the flow geometry is dominantly horizontal, compressional and Rayleigh wave velocities are high along the flow direction, and the velocities of horizontally polarized shear waves (SH) are faster than those of vertically polarized shear waves (SV) (*2–4*).

Deformation with a large strain causes LPO to form. At a usual tectonic stress level (~10 MPa or less), a large strain deformation occurs only at high temperatures. Thus, LPO and the resultant anisotropy in seismic-wave velocities in the shallow portions of the mantle where current temperature is low reflect the influence of the deformation mechanisms when these portions were hot, that is, during or soon after rifting, for example. The LPO in these depths is frozen as these portions are cooled down. In contrast, the LPO in the deeper mantle (>~200 km) reflects the deformation mechanism or mechanisms currently operating (*40*).

Measurements of LPO have been made on samples of the upper mantle to a depth of ~200 km (*45*). These values indicate that upper mantle rocks in this depth range and at a stress level of ~10 MPa (the typical stress thought to occur in the mantle) deform mostly by dislocation creep. However, some observations suggest that deformation in highly recrystallized rocks in the deep upper mantle (~200 km) is caused by diffusion (or superplastic) creep (*46*).

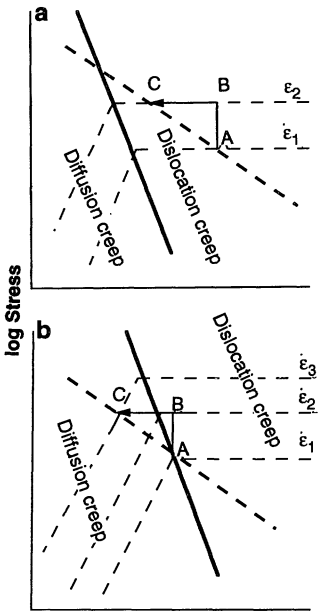

Fig. 4. Schematic diagrams showing the effects of stress increase and grain-size reduction on rheological behavior of olivine. A thick solid line represents the relation of stress to transition grain size (d_t), and a thick broken line shows the relation of recrystallized grain size (d_r) to stress. Thin broken lines show constant strain rate contours ($\dot{\epsilon}_1 < \dot{\epsilon}_2 < \dot{\epsilon}_3$). When stress increases, strain rate increases instantaneously ($\dot{\epsilon}_1 \rightarrow \dot{\epsilon}_2$) because of a larger driving force for the motion of relevant defects (A → B). However, in the dislocation-creep regime, a stress increase is followed by a change in grain size through dynamic recrystallization (B → C). (**a**) When this change occurs far from the transition condition between diffusion and dislocation creep, then grain-size reduction has no effect on strain rate. (**b**) However, when grain-size reduction occurs near the transition conditions, then the recrystallized grain size becomes smaller than the transition grain size, so that a significant rheological weakening results ($\dot{\epsilon}_2 \rightarrow \dot{\epsilon}_3$). Such grain-size reduction occurs, for example, at the initiation of continental rifting or when two plates collide.

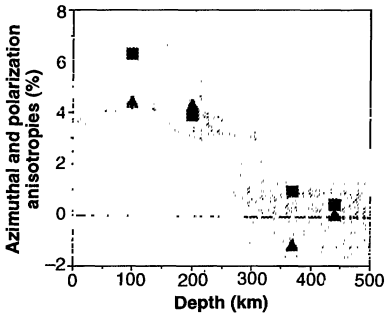

Fig. 5. Depth variation of amplitude of seismic anisotropy (*28*). Anisotropy of surface wave velocities can be observed either as the azimuthal variation of velocities or as the dependence of velocities on polarization. The (maximum) amplitude of azimuthal anisotropy of Rayleigh waves (filled squares) and the (average) amplitude of polarization anisotropy (filled triangles) [(SH-SV)/SH, where SH is the velocity of horizontally polarized shear waves and SV is the velocity of vertically polarized shear waves] are shown from Montagner and Tanimoto (*28*). Values in the figure for polarization anisotropy are 2 [(SH-SV)/SH]. A significant decrease in anisotropy occurs ~200 to 300 km. The results of Dziewonski and Anderson (*27*) show a significant anisotropy only in the upper ~200 km and are consistent with Montagner and Tanimoto's results (*28*).

Table 2. Rheological Earth models and ice models. The parameters refer to a creep law $\dot{\epsilon} = A^* \sigma^n$; NLZ nonlinear rheology zone.

Parameter	Model					
	A	B	C	D	E	F
Lithosphere thickness (km)	120	220	220	220	220	220
Thickness of NLZ (km)	100	100	0	450	Infinite	100
n in NLZ	3	3		3	3	3
n below NLZ	1	1	1	1	3	1
A^* in NLZ (Pa^{-n} s^{-1})	1×10^{-34}	1×10^{-34}		1×10^{-34}	1×10^{-34}	1×10^{-34}
n below NLZ	1	1	1	1	3	1
A^* in upper mantle below NLZ (Pa^{-n} s^{-1})	3×10^{-22}	3×10^{-22}	3×10^{-22}	3×10^{-22}	3×10^{-34}	3×10^{-22}
n in lower mantle	1	1	1	1	3	1
A^* in lower mantle (Pa^{-n} s^{-1})	3×10^{-22}	3×10^{-22}	3×10^{-22}	3×10^{-22}	3×10^{-34}	3×10^{-23}
Maximum ice thickness (m)	3500	3500	3500	3500	3500	1600
Time of deglaciation (1000 years)	12	12	12	12	8	12

Seismological observations of the shallow upper mantle are consistent with the observations of LPO that dislocation creep dominates in the uppermost mantle rocks (*2–4*). However, recent studies based on long-period surface waves indicate that the seismic anisotropy <200 to 300 km is significantly less than that at the shallower depths (*27, 28*) (Fig. 5). This observation suggests that the dominant deformation mechanism may change from dislocation creep in the shallow upper mantle to diffusion creep in the deep upper mantle. An observed seismic discontinuity at ~200 km (the Lehmann discontinuity) may result from a change in LPO associated with a change in deformation mechanisms (*47*). Thus, the observed LPO and the anisotropy of seismic wave velocities provide strong evidence that dislocation creep is the dominant mechanism of flow in the shallow upper mantle when it is hot. However, some seismological observations (absence of anisotropy in the deep upper mantle and the Lehmann discontinuity at 200 to 300 km) suggest that the deformation mechanism in the deep upper mantle may be diffusion creep.

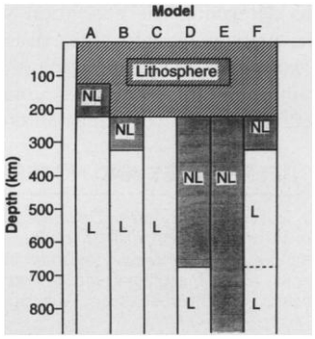

Fig. 6. Rheological models of the Earth's mantle. All models have an elastic lithosphere (diagonal lines) near the surface. Under the lithosphere, material behaves like a viscoelastic body whose rheology is either linear (L) or nonlinear (NL). Parameters in the models are summarized in Table 2, and letters A to F correspond to the models therein.

Rheological Weakening and Shear Localization

The upper mantle in or near the depth of rheological transition weakens as stress increases. Geological conditions under which the stress in the upper mantle increases with time include the initiation of continental rifting, possibly as a result of the collision of plume head with the bottom of continental lithosphere (*48*), and the collision of continents. In a typical part of the upper mantle away from the mid-ocean ridge environment, the dominant deformation mechanism is diffusion creep in the shallow upper mantle (down to near the base of the lithosphere) and in the deep upper mantle (in the deep asthenosphere). However, the dominant mechanism is dislocation creep in the intermediate depth (in the shallow asthenosphere) (Fig. 3). Upon a stress increase, there is an instantaneous increase in strain rate at a given initial grain size ($\dot{\epsilon}_1 \rightarrow \dot{\epsilon}_2$) (Fig. 4). As deformation proceeds [strain of >10 to 50% (*43*)], dynamic recrystallization reduces grain size. When this reduction in grain size occurs under the conditions of regions far from the transition, strain rate remains essentially unchanged (Fig. 4a). However, under conditions of areas near the transition, the grain size may become small enough to promote diffusion creep; if so, the mantle weakens significantly ($\dot{\epsilon}_2 \rightarrow \dot{\epsilon}_3$) (Fig. 4b). The soft rheology persists only temporarily, however, because of the grain growth that occurs in the diffusion creep regime.

We suggest that the upper mantle just below the shallow transition depth and above the deep transition depth undergoes rheological weakening when stresses increase. As a result, deformation is localized, and the parts of the mantle above and below the transition depths become mechanically decoupled. Such a possibility in the shallow continental upper mantle (just below the Moho, that is, at a depth of 20 to 50 km) was suggested on the basis of experimental data on olivine rheology (*9*). The role of diffusion creep in enhancing continental rifting was also proposed (*49*). On the basis of recent laboratory studies and the observation of seismic anisotropy, we propose that similar weakening and resultant mechanical decoupling may occur also in the deep upper mantle (200 to 300 km) (*50*).

Postglacial Rebound and Upper Mantle Rheology

Theoretical analysis of the vertical crustal movement after the last deglaciation (8,000 to 12,000 years ago) near the deglaciated regions also helps to define constraints on the stress dependence of flow (*51*). Crustal uplift near the deglaciated region is sensitive to stress dependence of flow (*52*) because the stress magnitude in this region changes both temporally and spatially, and so the flow pattern there depends significantly on the stress sensitivity of flow (*25*). When the rheology is nonlinear, the initial flow of materials to the interior of the deglaciated region is fast because of high stress, and this flow diminishes rapidly with time. Therefore, emergence near the edge of the ice sheet results. In contrast, when the rheology is linear, the flow is not fast initially and the peripheral bulge migrates inward.

We have tested several models of mantle rheology and found that the observation of postglacial rebound is compatible with a model in which the viscoelastic response is dominated by linear rheology; only a thin (<200 km) nonlinear rheological layer is consistent with the observed crustal uplift. The model of the Earth used in this study is composed of several homogeneous layers with different mechanical properties (Fig. 6 and Table 2). The top layer is the lithosphere and was taken to be elastic with respect to the time scale of postglacial rebound. Also, because the lithosphere is considered elastic, it does not matter whether the dominant creep mechanism is dislocation or diffusion creep. The underly-

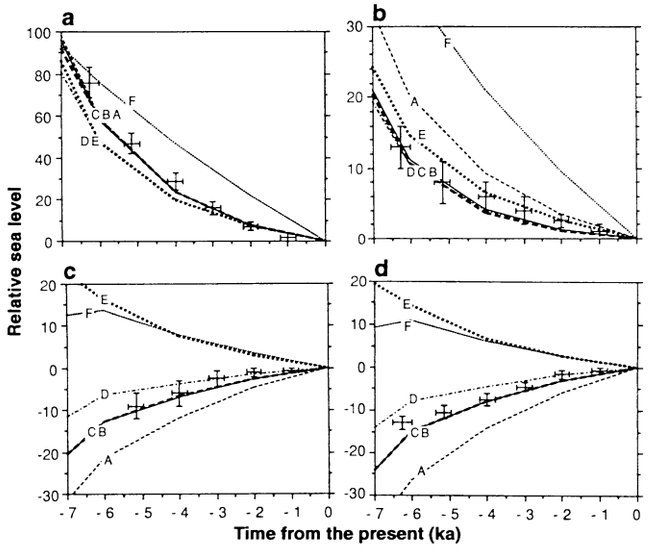

Fig. 7. Comparison of the observed RSL data with the values predicted by models A to F (Fig. 6 and Table 2) at four sites that range from (**a**) near the center of rebound (Ottawa Island) and (**b**) near the edge of the load but still inside the ice sheet (northwest Newfoundland) to (**c** and **d**) sites just outside the edge of the ice sheet (Boston and Delaware, respectively). Letters correspond to the values of their respective models. Radiocarbon age of the data has been converted to sidereal age, as in (*62*); ka, thousands of years ago. The results indicate that only a thin (<200 km), nonlinear layer is compatible with the observed RSL data.

ing layers were viscoelastic. The elastic parameters of these layers were determined seismologically—only the rheologies of these layers were allowed to vary. We consider six models of rheology: The reference model (model C) had a uniform mantle with a linear rheology. Models A and B had a thin (100 km) layer of nonlinear rheology with a thin (120 km) and a thick (220 km) lithosphere for models A and B, respectively. Model D has a thick lithosphere and a thick (450 km) layer of nonlinear rheology. Model E has a thick lithosphere and an underlying layer with uniform nonlinear rheology. Model F is similar to model B, but its viscosity is assumed to increase by a factor of 10 at the 670-km discontinuity.

The comparison between the observed RSL and those predicted by the Earth models is shown in Fig. 7 (*53*). The sea level values from models with a thin or no nonlinear layer and a thick lithosphere (for example, models B and C) fit the data equally well. But a model with a thin lithosphere (model A) fits poorly with the observed RSL in Boston, Delaware, and northwest Newfoundland, which suggests a thick lithosphere in this region (*54*). Because of the stationary behavior of the peripheral bulge, data from models with a thick nonlinear layer (models D and E) fit poorly with the observations at Boston and Delaware, indicating that much of the nonelastic deformation responsible for the postglacial crustal uplift is due to deformation with a linear rheology. A poor fit of model F indicates that a significant increase in viscosity in the lower mantle is not possible in this region (*55*).

Theoretical modeling of the postglacial rebound indicates that the Earth's mantle behaves mostly like a linear viscoelastic body, consistent with a model with only a thin (<200 km) layer of nonlinear rheology. Some rheological features such as a thick lithosphere and a small contrast in viscosity between the upper and lower mantle may be regional rather than global features because the geothermal gradient in the Laurentide region is small compared with those of other regions (*54*). However, the stress dependence of rheology that is inferred from this study appears to be applicable to other long-term tectonic processes such as mantle convection because the stress magnitudes in the two processes are similar (*52*).

Rheological Transitions and Their Implications for Mantle Dynamics

The upper mantle that deforms with a single mechanism is not compatible with all of the available geophysical observations. The observed significant anisotropy in seismic waves in the shallow upper mantle indicates that the deformation mechanism there must be dislocation creep when this region is hot and, hence, the rheology is nonlinear. In contrast, the analysis of the postglacial rebound provides a strong case for dominantly linear rheology. A working hypothesis to resolve this apparent contradiction includes a transition (or transitions) in deformation mechanisms with depth. On the basis of laboratory data on diffusion and creep, we have shown that the transitions in deformation mechanisms likely occur in the shallow upper mantle (a few tens of kilometers deep, depending on the geothermal gradient) and in the deep upper mantle (200 to 300 km). The depths of these transitions are not well constrained because of the large uncertainties involved in the extrapolation of laboratory data. However, the deeper transition depth may be tentatively identified with the Lehmann discontinuity (*47*), in which case it varies from 200 to 300 km depending on the tectonic setting (*56*).

Transition in the shallow upper mantle occurs at low temperatures and so causes a significant effect only when high stress is involved. In the collision zones where the stress is exceedingly high (≥100 MPa) (*57*), grain-size reduction promotes diffusion creep in the shallow portions of the upper mantle. Continental rifting may also be associated with a change in deformation mechanisms and the resultant rheological weakening (*49*). In contrast, rheological transition at the deeper upper mantle occurs at any tectonic stress. Thus the transition is global, although the depth of transition varies according to regional geothermal gradient, water content, or both (*47*).

Proposed rheological transitions and their related weakening have important geological and geophysical implications. Rheological weakening may promote such geological processes as continental rifting (*49*) or the deformation of continental lithosphere associated with continental collision. Mechanical decoupling causes a change in flow pattern above and below this transition. A recent result of high-resolution seismic tomography indicates that the pattern of heterogeneity differs significantly between the shallow upper mantle and the deep upper mantle (*28, 58*). A marked kink in geotherms is often observed at a depth of ~200 km in the studies of geothermal gradients that are based on element partitioning in mantle minerals (*18, 59*). This feature may also be caused by a change in flow pattern, flow velocity, or both, of an upwelling diapir as it passes through the rheological transition (*60*). The proposed change in deformation mechanisms represents a natural way to yield a nearly depth-independent viscosity in the deep upper mantle. With a much higher activation volume reported for dislocation creep, one would expect unreasonably high viscosities in the deep upper mantle (*61*).

Additional evidence is still needed to corroborate the notion of rheological transitions. First, LPO measurements of mantle xenoliths would be useful to delineate the deformation mechanisms in the deep interior of the Earth. In particular, the proposed layer of linear rheology in the lithosphere and deep asthenosphere (>200 to 300 km) can be tested by measurement of LPOs of xenoliths from appropriate depths. Deeper (>300 km) xenoliths (*19*), for example, show a weak LPO if the dominant deformation mechanism there is diffusion creep. Second, a detailed seismic survey to detect changes in anisotropy in the lithosphere and in the deep asthenosphere (200 to 300 km) would be useful to detect a change in deformation mechanisms. Third, deformation experiments under high pressures to determine the activation volume (and its pressure variation) in dislocation creep would be useful in placing tighter constraints on the transition conditions between dislocation and diffusion creep.

REFERENCES AND NOTES

1. H. J. Frost and M. F. Ashby, *Deformation Mechanism Maps* (Pergamon, Oxford, 1982).
2. S. Karato, in *High-Pressure Research in Mineral Physics*, M. H. Manghnani and Y. Syono, Eds. (American Geophysical Union, Washington, DC, 1987), pp. 455–471.
3. _____, in *Rheology of Solids and of the Earth*, S. Karato and M. Toriumi, Eds. (Oxford Univ. Press, Oxford, 1989), pp. 393–422.
4. A. Nicolas and N. I. Christensen, in *Composition, Structure and Dynamics of the Lithosphere-Asthenosphere System*, K. Fuchs and C. Froidevaux, Eds. (American Geophysical Union, Washington, DC, 1987), pp. 111–123.
5. U. R. Christensen, *Geophys. J. R. Astron. Soc.* **91**, 711 (1987).
6. Two major processes of preferred orientation development, namely, rotation of crystallographic lattice as a result of slip and migration of grain boundaries driven by heterogeneity in dislocation densities, operate only in the dislocation creep regime [S. Karato, *Phys. Earth Planet. Inter.* **51**, 107 (1988)]. Some changes in preferred orientation may occur near the transition conditions between dislocation and diffusion creep. Near the transition conditions, deformation occurs by both diffusive mass transport and dislocation motion, and so only the soft-slip system or systems of dislocations are needed. In contrast, under the conditions far from the transition where only dislocation motion can contribute to strain, various slip systems are needed to achieve large strain deformation of polycrystalline materials [for example, J. Gill Sevillano, P. van Houtte, E. Aernoudt, *Prog. Mater. Sci.* **25**, 69 (1981)]. Therefore, the resultant preferred orientation may be different between the two conditions, but the nature of preferred orientation near the transition conditions is not well understood.
7. D. A. Yuen and G. Schubert, *J. Geophys. Res.* **81**, 2499 (1976).
8. U. R. Christensen and D. A. Yuen, *ibid.* **94**, 814 (1989); P. A. van der Berg, D. A. Yuen, P. E. van Keken, *Geophys. Res. Lett.* **18**, 2197 (1991).
9. S. H. Kirby, *Tectonophysics* **119**, 1 (1985); E. H. Rutter and K. H. Brodie, *Geol. Rundsch.* **77**, 295 (1988).

10. S. Karato, *Phys. Earth Planet. Inter.* **24**, 1 (1981); G. Ranalli, in *Glacial Isostasy, Sea-Level and Mantle Rheology*, R. Sabadini, K. Lambeck, E. Boschi, Eds. (Kluwer Academic, Dordrecht, the Netherlands, 1991), pp. 343–378.
11. N. L. Carter and H. G. Ave'Lallemant, *Geol. Soc. Am. Bull.* **81**, 2181 (1970); D. L. Kohlstedt and C. Goetze, *J. Geophys. Res.* **79**, 2045 (1974); W. B. Durham and C. Goetze, *ibid.* **82**, 5737 (1977).
12. S. H. Kirby and A. K. Kronenberg, *Rev. Geophys.* **25**, 1219 (1987); S. J. Mackwell, Q. Bai, D. L. Kohlstedt, *Geophys. Res. Lett.* **17**, 9 (1990).
13. The major difficulty is the measurement of deviatoric stress under high pressures and high temperatures. The most reliable technique is the use of a load cell (a stress-measuring device) in the high-pressure environment. But this approach has been used only for pressures <~500 MPa in an apparatus where a gas is used to generate a high pressure. At higher pressures, solids are usually used as pressure-generating media, and the use of an internal load cell is difficult. When the deviatoric stresses are measured outside the high-pressure assembly, a large correction for friction must be made that causes significant uncertainties in the measurement of material strength. Although a relatively low friction specimen assembly has been developed and applied at pressures <3 GPa (*14*), the uncertainties in stress measurements are considerably larger than those involved in the deformation experiments that use a gas-medium apparatus.
14. H. W. Green II and R. S. Borch, *Acta Metall.* **36**, 1301 (1987).
15. R. B. Gordon, *J. Geophys. Res.* **70**, 2413 (1965); R. L. Stocker and M. F. Ashby, *Rev. Geophys. Space Phys.* **11**, 391 (1973); G. Ranalli and B. Fischer, *Phys. Earth Planet. Inter.* **34**, 77 (1984).
16. S. Karato, M. S. Paterson, J. D. Fitz Gerald, *J. Geophys. Res.* **91**, 8151 (1986).
17. H. W. Green II and S. V. Radcliff, *Earth Planet. Sci. Lett.* **15**, 239 (1972); Y. Gueguen, *Tectonophysics* **39**, 231 (1977); Z.-M. Jin, H. W. Green II, R. S. Borch, *ibid.* **169**, 23 (1989).
18. The temperature and pressure dependence of the partitioning of elements, between coexisting minerals has been used to estimate the depth from which inclusions of upper-mantle rocks in some volcanic rocks are carried away; F. R. Boyd, *Geochim. Cosmochim. Acta* **37**, 2533 (1973).
19. Although rare, some "ultradeep" upper mantle rocks have been found from South Africa in which the silica content in garnets is unusually high, suggesting a depth >300 km; S. E. Haggerty and V. Sautter, *Science* **248**, 993 (1990).
20. C. Goetze, *Geology* **3**, 172 (1975).
21. W. R. Peltier, P. Wu, D. A. Yuen, in *Anelasticity of the Earth*, vol. 4 of *Geodynamics Series*, F. D. Stacey, M. S. Paterson, A. Nicolas, Eds. (American Geophysical Union, Washington, DC, 1981), pp. 59–77; A. M. Tushingham and W. R. Peltier, *J. Geophys. Res.* **97**, 3285 (1992).
22. Effective viscosity η is defined as $\sigma/2\dot{\epsilon}$, where σ is the stress and $\dot{\epsilon}$ is the strain rate. Effective viscosity for a linear rheology is independent of stress or strain rate, but effective viscosity for nonlinear rheology depends on stress or strain rate.
23. Another controversial issue is the depth variation of viscosity. Nearly isoviscous mantle [for example, L. M. Cathles, *The Viscosity of the Earth's Mantle* (Princeton Univ. Press, Princeton, NJ, 1975), p. 386] and a significant increase in viscosity with depth [M. Nakada and K. Lambeck, *Geophys. J.* **96**, 497 (1989)] have been proposed on the basis of analysis of postglacial crustal uplift.
24. R. L. Post, Jr., and D. T. Griggs, *Science* **181**, 1242 (1973); S. T. Crough, *Geophys. J. R. Astron. Soc.* **50**, 723 (1977); T. Yokokura and M. Saito, *J. Phys. Earth* **26**, 147 (1978); M. Nakada, *ibid.* **31**, 349 (1983).
25. P. Wu, *Geophys. J.* **108**, 35 (1992).
26. Diffusion coefficients of the slowest diffusing species in olivine were estimated from the rate of dislocation recovery under high temperature (T < 1500°C) and high pressures (P < 10 GPa); S. Karato, D. C. Rubie, H. Yan, *J. Geophys. Res.*, in press.
27. A. M. Dziewonski and D. L. Anderson, *Phys. Earth Planet. Inter.* **25**, 297 (1981).
28. J.-P. Montagner and T. Tanimoto, *J. Geophys. Res.* **96**, 20337 (1991).
29. A. E. Ringwood, *Composition and Petrology of the Earth's Mantle* (McGraw-Hill, New York, 1975), p. 618.
30. J. V. Ross and K. C. Nielsen, *Tectonophysics* **44**, 233 (1978); S. J. Mackwell, *Geophys. Res. Lett.* **18**, 2027 (1991).
31. H. G. Ave'Lallemant, J.-C.-C. Mercier, N. L. Carter, J. V. Ross, *Tectonophysics* **70**, 85 (1980); A. Nicolas, *Rev. Geophys.* **24**, 875 (1986); G. Ceulenner, A. Nicolas, F. Boudier, *Tectonophysics* **151**, 1 (1988).
32. The rate-controlling step in diffusion creep and in dislocation recovery is the diffusion of the slowest diffusing species, namely, oxygen or silicon in olivine. Thus, the activation volume should be the same between the two processes, except for possible minor differences caused by the contribution of jog formation volume (the volume necessary to form a step on the dislocation line). A possible complication is the role of grain-boundary diffusion in diffusion creep. If mass transport through grain boundaries is important, the results of dislocation recovery, which are related to diffusion through grains (bulk diffusion), cannot be used in the calculation of diffusion creep. On the assumption of the theoretical relation $V^* \sim AE^*$, in which A is a parameter that depends on elastic constants, a dielectric constant, and their pressure derivatives [S. Karato, *Phys. Earth Planet. Inter.* **25**, 38 (1981)], the activation volume for grain-boundary diffusion should be smaller than that for bulk diffusion, because activation energy for grain-boundary diffusion is smaller than for bulk diffusion. Thus, the occurrence of creep from grain-boundary diffusion in the upper mantle would support our conclusion that rheological transitions occur as a result of differences in temperature and pressure dependence between diffusion and dislocation creep.
33. Two papers have been published regarding the activation volume for dislocation creep in olivine. J. V. Ross, H. G. Ave'Lallemant, and N. L. Carter [*Science* **203**, 261 (1979)] measured the pressure dependence of creep in olivine polycrystals (in the dislocation creep regime) using a solid medium high-pressure deformation apparatus at up to 1.5 GPa with talc as a confining medium. Because talc is decomposed to provide water at high temperatures, the conditions of these experiments were wet (water-saturated). They obtained the activation volume of 13 $cm^3\ mol^{-1}$. This result has large uncertainties because of the difficulties in the measurement of strength at high pressures (*13*). Green and Borch (*14*) developed a liquid medium specimen assembly for rock deformation and determined the pressure dependence of creep in polycrystalline olivine in the dislocation creep regime up to 3 GPa. The specimens were polycrystalline olivine aggregates that were prepared by hot-pressing. Because the starting material was natural dunite from Balsam Gap that had not been dried at high temperatures, the specimens should have contained some hydrous minerals that provide water at high temperatures. However, the amount of water was significantly less than that in Ross, Ave'Lallemant, and Carter's study because the specimens were in the platinum jacket that was surrounded by molten NaCl, which sucks water from the surroundings. Green and Borch obtained an activation volume of 27 $cm^3\ mol^{-1}$ under this moderately dry but poorly defined condition. R. S. Borch and H. W. Green II [*Nature* **330**, 345 (1987)] proposed that the activation volume of creep in olivine may decrease significantly with pressure. However, the range of pressure explored in this study was too small (<3 GPa) to justify this notion (*61*).
34. E. Ito, D. M. Harris, A. T. Anderson, Jr., *Geochim. Cosmochim. Acta* **47**, 1613 (1983).
35. D. R. Bell and G. R. Rossman, *Science* **255**, 1391 (1992).
36. Q. Bai and D. L. Kohlstedt, *Nature* **357**, 672 (1992).
37. S. Karato, *ibid.* **347**, 272 (1990).
38. G. Heinson and S. Constable, *Geophys. J.* **110**, 159 (1992).
39. Viscosities, η_o, are calculated for a reference stress (σ_o = 1 MPa) and grain size (d_o = 1 mm) which are assumed to be independent of depth. The viscosity, η, at different stress, σ, different grain size, d, or both, can be calculated from
$$\eta/\eta_o = (d/d_o)^m(\sigma/\sigma_o)^{1-n}$$
where n is the stress exponent and m is the grain-size exponent (see Table 1).
40. S. Karato, *Tectonophysics* **104**, 155 (1984).
41. The driving force for grain growth is grain-boundary energy, which is present in both dislocation creep and diffusion creep regimes. The driving force for dynamic recrystallization is dislocation energy, which is present in a significant amount only in the dislocation creep regime.
42. When grain growth occurs, grain size increases with time [S. Karato, *Tectonophysics* **168**, 255 (1989)], but grain size is eventually fixed at a certain stable size, which is determined by the fraction and size of secondary-phase particles [D. L. Olgaard and B. Evans, *J. Am. Ceram. Soc.* **69**, C-272 (1986)].
43. S. Karato, M. Toriumi, T. Fujii, *Geophys. Res. Lett.* **7**, 649 (1980). The theoretical basis for the relation between recrystallized grain size and stress is not well understood. Grain size is presumably determined by the dynamic balance between the grain coarsening process (grain growth) and grain refinement due to deformation [B. Derby, *Acta Metall.* **39**, 955 (1991)]. In this relation, a weak dependence of grain size on thermodynamic variables (such as temperature, pressure, and water fugacity) is expected.
44. Because the slopes of the transition grain size d_t versus stress and recrystallized grain size d_r versus stress curves are nearly the same, the results in Fig. 3, B, D, and F, are sensitive to creep law parameters and the recrystallized grain-size and stress relations (Eq. 2) and so are subject to large uncertainties.
45. J.-C.-C. Mercier, in *Preferred Orientation in Deformed Metals and Rocks: An Introduction to Modern Texture Analysis*, H.-R. Wenk, Ed. (Academic Press, New York, 1985), pp. 407–430.
46. A. M. Boullier and Y. Gueguen, *Contrib. Mineral. Petrol.* **50**, 93 (1975).
47. S. Karato, *Geophys. Res. Lett.* **19**, 2255 (1992).
48. R. I. Hill, *Earth Planet. Sci. Lett.* **104**, 398 (1991).
49. J. R. Hopper and W. R. Buck, *J. Geophys. Res.*, in press.
50. Weakening and resultant mechanical decoupling at ~200 km were proposed to result from the proximity of the geotherm to the melting point [J. H. Leven, I. Jackson, A. E. Ringwood, *Nature* **289**, 234 (1981)].
51. In the interpretation of RSL data, one must consider the relation between ice sheet melting history and mantle rheology [(*21*); P. Wu and W. R. Peltier, *Geophys. J. R. Astron. Soc.* **74**, 377 (1983)]. For data away from the ice sheet, the effect of the ice melting history is small. The use of RSL data near the edge of the ice sheet to constrain the definition of mantle rheology is questionable because RSL data, which are also sensitive to the melting history of ice sheets, are not well constrained in the Laurentide [M. Nakada and K. Lambeck, *Geophys. J.* **89**, 171 (1987); K. Lambeck, *Q. J. R. Astron. Soc.* **31**, 1 (1990)]. However, the uncertainties in melting history have had a smaller effect on the examination of temporal variation of RSL during the last 7,000 years because the ice had left the mantle at least 10,000 years ago.
52. Deformation associated with the postglacial rebound near the deglaciated regions is associated with a stress magnitude of 1 to 5 MPa in the upper mantle (*25*). This magnitude is on the same order as that associated with mantle convection [for example, F. D. Stacey, *Physics of the Earth* (Brookfield, Brisbane, Australia, 1992),

chap. 6]. Thus, deformation mechanisms for the postglacial rebound in the upper mantle near the deglaciated region are similar to those involved in mantle convection. A large difference between the two processes is the strain magnitude. Strain involved in the postglacial rebound is small ($\sim 10^{-5}$), and transient rather than steady-state creep might occur [J. Weertman, *Philos. Trans. R. Astron. Soc. London Ser. A* **288**, 9 (1978)]. However, recent analysis of transient creep in olivine suggests that the transient period in olivine is much shorter than that of most metals, and so the transient creep proposed by Weertman may not be important [S. Karato, in (*3*), pp. 176–208].

53. The ice sheet was interpreted to have a parabolic profile. The ice thickness at the load center and the time of deglaciation were adjusted to give the best fit to the RSL data at the center of the load. A thickness of 3500 m was chosen in models A, B, C, D, and E and a thickness of 1600 m was chosen in model F. We chose a deglaciation time of 12,000 years before present except in model E, where 8,000 years before present was chosen. For each model, the first-order approximations to the sea level equations were solved, with the effects of eustatic sea level change, unloading of the ice, and loading of the ocean floor taken into account. As demonstrated by Wu and Peltier in (*51*), such an approximation is valid for RSL in the last 7000 years.
54. This result is consistent with that of W. R. Peltier [*J. Geophys. Res.* **89**, 11303 (1984)], who used the RSL data in the Laurentide region, but not with that of M. Nakada and K. Lambeck [*Geophys. J. Int.* **96**, 497 (1989)], who used the RSL data in and near Australia where a much thinner lithosphere (50 to 100 km) was inferred. This discrepancy may be due in part to the difference in the geothermal gradient between the two regions, because the recent high-resolution seismic tomography indicates a colder upper mantle in the Laurentide than in Australia [D. L. Anderson, T. Tanimoto, Y.-S. Zhang, *Science* **256**, 1645 (1992)].
55. This observation is consistent with some of the findings of Peltier, Wu, and Yuen in (*21*) but not with those of Nakada and Lambeck in (*23*). Part of this discrepancy may result from the regional difference in geothermal regimes (*54*).
56. J. Revenaugh and T. H. Jordan, *J. Geophys. Res.* **96**, 19781 (1991).
57. D. L. Kohlstedt and M. S. Weathers, *ibid.* **85**, 6269 (1980).
58. Y.-S. Zhang and T. Tanimoto, *Nature* **355**, 45 (1992).
59. T. Kawasaki, *Lithos* **20**, 263 (1987).
60. P. van Keken, D. A. Yuen, A. van den Berg, *Earth Planet. Sci. Lett.* **112**, 179 (1992).
61. An alternative way to get nearly isoviscous upper mantle with a large activation volume is to invoke a large decrease in activation volume with pressure. Borch and Green in (*33*) proposed that in the relation between strain rate and temperature and pressure

$$\dot{\epsilon} = A\sigma^n \exp[-gT_m(P)/T]$$

in which g is a constant and $T_m(P)$ is the melting temperature, this second variable should be identified as the solidus rather than the melting temperature of the constituting mineral or minerals. The solidus of peridotite changes with pressure with a large curvature [E. Takahashi, *J. Geophys. Res.* **91**, 3985 (1986)], and so the presence of nearly isoviscous upper mantle would be interpreted from this assumption. However, this assumption contradicts the experimental observations. If the solidus rather than the melting temperature determines rheology, then creep rate in olivine should increase by a factor of 10^4 to 10^5 when a small amount of pyroxenes is added, because the solidus will be reduced by 500 to 600 K. The observed increase in strain rate by the addition of orthopyroxene is only a factor of about 3 [Q. Bai, S. J. Mackwell, D. L. Kohlstedt, *J. Geophys. Res.* **96**, 2441 (1991)]. Therefore, the change in activation volume with pressure under the upper mantle conditions appears to be small, and so an activation volume as high as 27 $cm^3\ mol^{-1}$ leads to unacceptably high viscosities in the deep upper mantle (Fig. 2).
62. Sidereal age is based on the sidereal day—the time required for the Earth to rotate once about its axis; E. Bard, B. Hamelin, R. G. Fairbanks, A. Zindler, *Nature* **345**, 405 (1990).
63. We thank D. A. Yuen, W. R. Peltier, and D. L. Kohlstedt for reading the manuscript and for stimulating discussions. Supported by the National Science Foundation (EAR-9017811) (S.K.) and by the Natural Sciences and Engineering Research Council (Canada) (P.W.).

RESEARCH ARTICLE

Structure-Specific Endonucleolytic Cleavage of Nucleic Acids by Eubacterial DNA Polymerases

Victor Lyamichev,* Mary Ann D. Brow, James E. Dahlberg†

Previously known 5′ exonucleases of several eubacterial DNA polymerases have now been shown to be structure-specific endonucleases that cleave single-stranded DNA or RNA at the bifurcated end of a base-paired duplex. Cleavage was not coupled to synthesis, although primers accelerated the rate of cleavage considerably. The enzyme appeared to gain access to the cleavage site by moving from the free end of a 5′ extension to the bifurcation of the duplex, where cleavage took place. Single-stranded 5′ arms up to 200 nucleotides long were cleaved from such a duplex. Essentially any linear single-stranded nucleic acid can be targeted for specific cleavage by the 5′ nuclease of DNA polymerase through hybridization with an oligonucleotide that converts the desired cleavage site into a substrate.

Important functions of several DNA polymerases (DNAPs) include the removal of nucleotides from the 5′ and 3′ ends of DNA chains (*1*). For example, the 5′ exonuclease activities located in the NH_2-terminal domains of DNAP from *Escherichia coli* (DNAP-Ec1) and *Thermus aquaticus* (DNAP-Taq) can participate in (i) removal of the RNA primers of lagging strand synthesis during replication and (ii) the removal of damaged nucleotides during repair (*1*, *2*). Although mononucleotides predominate among the digestion products, short oligonucleotides (≤12 nucleotides) can also be observed, implying that these so-called 5′ exonucleases can function endonucleolytically (*3*, *4*). Thus, we like to call these activities 5′ nucleases.

For removal of primers or damaged nucleotides, a 5′ nuclease must be able to cleave RNA and DNA strands regardless of their sequences. However, indiscriminate cleavage of the nucleic acids would be lethal. We propose that this problem is resolved by having the 5′ nuclease recognize its substrate by structure rather than sequence. An appropriate structure would be the junction where the two strands of a duplex separate into single-stranded arms; the arm with a free 5′ end would be recognized as the displaced strand that is to be cleaved from the remaining duplex (Fig. 1A). To avoid ambiguity, we refer to the top and bottom strands of the complex as the substrate and template strands, respectively. A primer that would be extended during nick translation is paired to the 3′ arm of the template strand. To test our model of recognition and cleavage by the 5′ nuclease, we used the substrate and template strands shown in Fig. 1A, covalently joined at the end of the duplex, for experimental convenience. We also used this model to develop a method for cleaving single-stranded nucleic acids efficiently at desired sites with extreme sequence specificity.

The 5′ nuclease of DNAP-Taq. Incubation of the structure shown in Fig. 1A with DNAP-Taq (*5*) and deoxynucleoside triphosphates (dNTPs) resulted in the re-

The authors are in the Department of Biomolecular Chemistry, University of Wisconsin School of Medicine, 1300 University Avenue, Madison, WI 53706.

*On leave from the Institute of Molecular Genetics, Moscow, Russia.
†To whom correspondence should be addressed.